

Vibronic Coupling and Single-Step Energy Transfer in the System $\text{Na}_5(\text{Gd}, \text{Eu})(\text{WO}_4)_4$

J. P. M. VAN VLIET AND G. BLASSE*

*Physics Laboratory, University of Utrecht, P.O. Box 80 000,
3508 TA Utrecht, The Netherlands*

Received June 5, 1989

The luminescence properties of the system $\text{Na}_5(\text{Gd}, \text{Eu})(\text{WO}_4)_4$ are reported. The intensity of the vibronic sidebands in the excitation spectra of the Eu^{3+} emission increases with the Eu^{3+} concentration, whereas in the emission spectra this intensity is concentration independent. This is explained tentatively with a model involving the 7F and charge-transfer states of Eu^{3+} and the charge-transfer state of WO_4^{2-} . Vibrational frequencies are derived from the spectra. Multistep energy migration over the Eu^{3+} sublattice is not observed in $\text{Na}_5\text{Eu}(\text{WO}_4)_4$. The luminescence of about 10% of the Eu^{3+} ions is quenched by single-step energy transfer to acceptors. Single-step energy transfer also occurs from WO_4^{2-} to Eu^{3+} . © 1990 Academic Press, Inc.

1. Introduction

The luminescence and energy migration properties of the Eu^{3+} ion in inorganic compounds have been the subject of extensive investigations in our laboratory (see, e.g., Refs. (1-4)). We reported on the luminescence of the double tungstates and molybdates of the composition $A\text{Eu}M_2\text{O}_8$ (A = alkali metal ion; M = Mo or W) (5). In these compounds energy migration is a relatively inefficient process. Also, we reported on the systems $\text{LiGd}_{1-x}\text{Eu}_x\text{F}_4$ and $\text{Gd}_{1-x}\text{Eu}_x\text{NbO}_4$ (6), in which energy migration occurs via Eu^{3+} - Eu^{3+} interactions of the exchange and, in the case of the niobate, superexchange type.

In this paper we report on the system $\text{Na}_5\text{Gd}_{1-x}\text{Eu}_x(\text{WO}_4)_4$ ($0 \leq x \leq 1$). The crystal structure of $\text{Na}_5\text{RE}(\text{WO}_4)_4$ (RE , rare-

earth ion), which has been described in Refs. (7, 8), is related to the scheelite structure of CaWO_4 . The RE site symmetry is the same as the cationic site symmetry in CaWO_4 , viz., S_4 . The shortest RE - RE distance is 6.5 Å, much larger than, for example, in RENbO_4 (3.8 Å), which also has a crystal structure that is closely related to the scheelite structure. In $\text{Na}_5\text{Eu}(\text{WO}_4)_4$ the Eu^{3+} nearest neighbors are linked via two O-W-O bridges. In this way every tungstate group has two Eu^{3+} neighbors located at about 3.9 Å from the center of the group. In contrast with $\text{NaEu}(\text{WO}_4)_2$, where the Na^+ and Eu^{3+} ions are randomly distributed over the bivalent cation sites of the scheelite structure, there is no cation disorder in $\text{Na}_5\text{Eu}(\text{WO}_4)_4$. The feature of the double O-M-O bridges (M , transition metal) between Eu^{3+} neighbors has also been encountered in $(\text{Gd}, \text{Eu})_2(\text{MoO}_4)_3$ (3). In this compound the bridges span a dis-

* To whom correspondence should be addressed.

tance of 6.3 Å between the Eu^{3+} ions. Nevertheless, energy transfer via superexchange was observed (3).

Considering the above, we studied the luminescence of $\text{Na}_5\text{Gd}_{1-x}\text{Eu}_x(\text{WO}_4)_4$ in order to get more information about the Eu^{3+} – Eu^{3+} transfer via exchange and superexchange interactions. The luminescence spectra have been analyzed before by Huang *et al.* (9), who performed crystal field calculations on $\text{Na}_5\text{Eu}(\text{MO}_4)_4$ (M , Mo, W). Evdokimov *et al.* (10) investigated the concentration quenching of the Eu^{3+} luminescence in $\text{Na}_5\text{La}_{1-x}\text{Eu}_x(\text{WO}_4)_4$ and $\text{Na}_5\text{Y}_{1-x}\text{Eu}_x(\text{WO}_4)_4$. Furthermore, room temperature luminescence measurements of a $\text{Na}_5\text{Eu}(\text{WO}_4)_4$ crystal have been reported by Pan *et al.* (11).

2. Experimental

Powder samples of composition $\text{Na}_5\text{Gd}_{1-x}\text{Eu}_x(\text{WO}_4)_4$ ($x = 0, 0.01, 0.2, 0.5, 0.7,$ and 1) were prepared using conventional solid state techniques. The starting materials (Na_2CO_3 , Merck z.A.; Gd_2O_3 and Eu_2O_3 , Highways Int. 99.999%; and WO_3 , Merck, reinst) were mixed and fired at 600°C for 5 hr. The structure of the samples was checked by X-ray powder diffraction.

3. Results

3.1. Spectral Properties

The excitation and emission spectra of $\text{Na}_5\text{Gd}(\text{WO}_4)_4$ at 20 K are given in Fig. 1. The excitation band has a maximum at about 230 nm. The emission band lies between 380 and 660 nm with a maximum at about 470 nm. From these data we find the Stokes shift to be about 22,000 cm^{-1} , which is larger than what has been found for CaWO_4 , viz. 18,000 cm^{-1} (14). The quenching temperature of the WO_4^{2-} emission is 200–250 K. In the excitation spectrum the $\text{Gd}^{3+} \ ^8S \rightarrow \ ^6I$ absorption line is visible as a

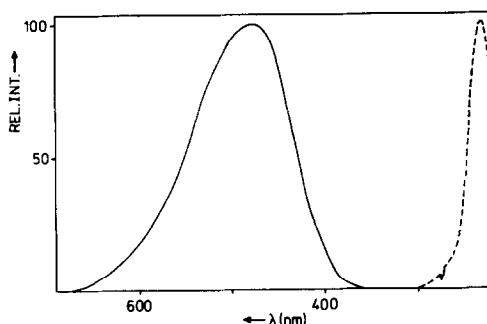


FIG. 1. Excitation (---) and emission (—) spectra of the WO_4^{2-} luminescence in $\text{Na}_5\text{Gd}(\text{WO}_4)_4$ at 20 K.

dip in the intensity of the WO_4^{2-} excitation band at 275 nm. Excitation at this wavelength yields Gd^{3+} emission ($^6P \rightarrow ^8S$ at 312 nm) as well as WO_4^{2-} emission.

All samples of the system $\text{Na}_5\text{Gd}_{1-x}\text{Eu}_x(\text{WO}_4)_4$ ($x \neq 0$) show a bright red Eu^{3+} luminescence upon irradiation with UV light at room temperature. Upon excitation into the 5L_6 level of Eu^{3+} ($\lambda_{\text{exc}} = 396$ nm), the sample with $x = 1$ exhibits the highest luminescence intensity, which means that concentration quenching of the Eu^{3+} emission is an inefficient process. This has also been observed by Evdokimov *et al.* (10) in the system $\text{Na}_5\text{La}_{1-x}\text{Eu}_x(\text{WO}_4)_4$.

Figure 2 presents the excitation spectrum of the Eu^{3+} emission of $\text{Na}_5\text{Eu}(\text{WO}_4)_4$ at 4.2 K. It consists of sharp lines in the spectral region 280–540 nm, corresponding to the electronic transitions within the $4f^6$ configuration of Eu^{3+} . Besides these lines, the WO_4^{2-} excitation band is present in the UV region of the spectrum, with a maximum at about 230 nm. Excitation in this band yields Eu^{3+} and WO_4^{2-} emission. In $\text{Na}_5\text{Eu}(\text{WO}_4)_4$ the amount of WO_4^{2-} emission is very small, only a small percentage of the total emission intensity. This indicates efficient $\text{WO}_4^{2-} \rightarrow \text{Eu}^{3+}$ energy transfer.

Furthermore some vibronic lines belonging to the $^7F_0 \rightarrow ^5D_{0,2}$ electronic transitions are observed. The intensity of these vibronics, compared to the intensity of the

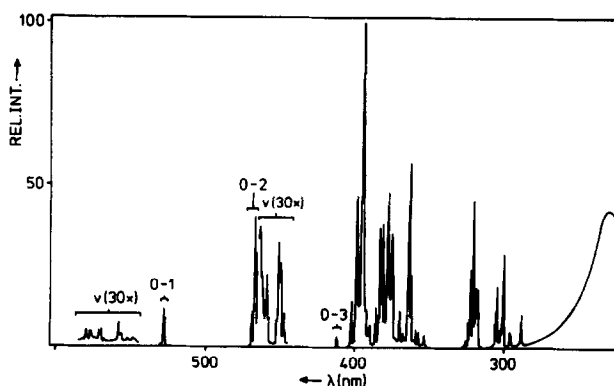


FIG. 2. Excitation spectrum of the Eu^{3+} emission of $\text{Na}_5\text{Eu}(\text{WO}_4)_4$, recorded at 4.2 K, $\lambda_{\text{em}} = 617$ nm. The notation $J-J'$ denotes the ${}^7F_J \rightarrow {}^5D_{J'}$ transitions of the Eu^{3+} ion. v , vibronic transition.

electronic ${}^7F_0 \rightarrow {}^5D_1$ magnetic dipole transition, increases with Eu^{3+} concentration in the dilution series. This can be seen in Table I which gives the ratio of the integrated vibronic intensity belonging to the ${}^7F_0 \rightarrow {}^5D_2$ transition and the intensity of the electronic ${}^7F_0 \rightarrow {}^5D_1$ transition.

Figure 3 gives the emission spectrum of $\text{Na}_5\text{Eu}(\text{WO}_4)_4$ at 4.2 K after excitation at 396 nm, i.e., into the 5L_6 level of Eu^{3+} . The sharp lines of the ${}^5D_0 \rightarrow {}^7F_{1,2,3,4}$ emission transitions are easily observable. Both the ${}^5D_0 \rightarrow {}^7F_1$ and the ${}^5D_0 \rightarrow {}^7F_2$ transition show a twofold splitting. Some vibronic emission lines occur in the spectral region 585–653 nm, belonging to the ${}^5D_0 \rightarrow {}^7F_0$ and ${}^5D_0 \rightarrow$

7F_2 transitions. The former electronic transition itself could not be observed in the emission spectra. As can be seen in Table I, the intensity of the vibronic lines in the emission spectra, again compared to the intensity of the ${}^5D_0 \rightarrow {}^7F_1$ magnetic dipole transition, is now independent of the Eu^{3+} concentration in the samples of the dilution series. From the energy difference between the vibronic and electronic transition in the excitation and emission spectra the vibra-

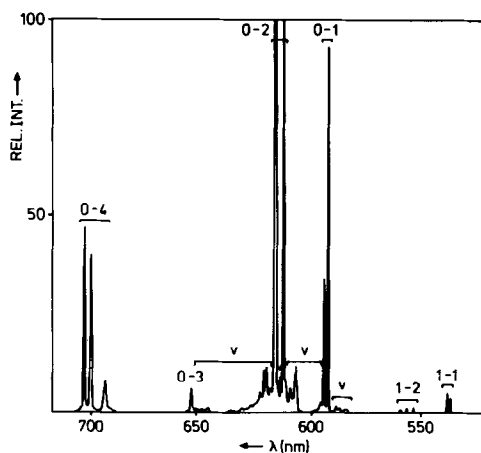


FIG. 3. Emission spectrum of $\text{Na}_5\text{Eu}(\text{WO}_4)_4$, recorded at 4.2 K, $\lambda_{\text{exc}} = 396$ nm. The notation $J-J'$ denotes the ${}^7F_J \rightarrow {}^5D_{J'}$ transitions of the Eu^{3+} ion. v , vibronic transition.

TABLE I

INTEGRATED INTENSITY RATIOS OF THE VIBRONIC AND ELECTRONIC TRANSITIONS I_v/I_e IN THE SPECTRA OF $\text{Na}_5\text{Gd}_{1-x}\text{Eu}_x(\text{WO}_4)_4$

x	Excitation spectrum ${}^7F_0 \rightarrow {}^5D_2/{}^7F_0 \rightarrow {}^5D_1$	Emission spectrum ${}^5D_0 \rightarrow {}^7F_2/{}^5D_0 \rightarrow {}^7F_1$
0.01	1.4	0.9
0.2	3.6	0.8
0.5	4.3	0.8
0.7	6.3	0.7
1	5.3	0.6

TABLE II
VIBRONIC LINES IN THE LUMINESCENCE SPECTRA OF $\text{Na}_5(\text{Gd}, \text{Eu})(\text{WO}_4)_4$ AT 4.2 K

Excitation spectra		Emission spectra		Assignment vibrational mode ^a
${}^7F_0 \rightarrow {}^5D_0$:	${}^7F_0 \rightarrow {}^5D_2$:	${}^5D_0 \rightarrow {}^7F_0$:	${}^5D_0 \rightarrow {}^7F_2$:	
17 210 + 60			16 190 - 60	} Lattice vibrations
17 210 + 140	21 460, 21 410 + 140	17 210 - 110	16 190 - 110	
	21 460, 21 410 + 210	17 210 - 150	16 190 - 130	} $\nu_2, \nu_4 (\text{WO}_4^{2-})$, i.e., W-O bending
17 210 + 300	21 460, 21 410 + 280	17 210 - 210	16 190 - 190	
17 210 + 350	21 460, 21 410 + 370	17 210 - 270	16 190 - 280	
			16 190 - 350	} $\nu_1, \nu_3 (\text{WO}_4^{2-})$, i.e., W-O stretching
17 210 + 730	21 460, 21 410 + 710	17 210 - 710	16 190 - 400	
17 210 + 780	21 460, 21 410 + 760	17 210 - 770	16 190 - 770	
		17 210 - 840	16 190 - 890	
		17 210 - 890	16 190 - 890	
17 210 + 940	21 460, 21 410 + 940	17 210 - 950	16 190 - 940	

Note. All Values in cm^{-1} .

^a By comparing with data given in Ref. (15).

tional frequencies involved in the vibronic transitions can be derived. These data are collected in Table II.

3.2. Decay Measurements

To obtain information about the time-dependent behavior of the Eu^{3+} emission we recorded the decay curves of the Eu^{3+} emission of $\text{Na}_5\text{Gd}_{0.99}\text{Eu}_{0.01}(\text{WO}_4)_4$ and $\text{Na}_5\text{Eu}(\text{WO}_4)_4$. This was performed by exciting the lowest 5D_1 crystal field level of

the Eu^{3+} ion at 527.62 nm and monitoring the ${}^5D_0 \rightarrow {}^7F_2$ emission line at 617.64 nm.

The decay curves of the diluted and concentrated sample have been measured at temperatures between 4.2 K and room temperature. All curves are initially nonexponential and have an exponential tail with a decay time of 760 μsec . Some representative results are given in Fig. 4.

4. Discussion

4.1. Spectral Properties

In $\text{Na}_5\text{Eu}(\text{WO}_4)_4$ the Eu^{3+} ion occupies a site with symmetry S_4 . The experimental and expected numbers of lines in the electronic ${}^7F_0 \rightarrow {}^5D_J$ and ${}^5D_0 \rightarrow {}^7F_J$ transitions are given in Table III. From this table it becomes clear that the experimental results do not violate the crystallographic site symmetry S_4 , but also that the higher site symmetry D_{2d} seems to be a very good approximation of the real site symmetry. In fact, this has also been remarked by Efremov *et al.* (8) and Huang *et al.* (9). The latter concluded this from their emission spectra and used the D_{2d} site symmetry in crystal field parameter calculations.

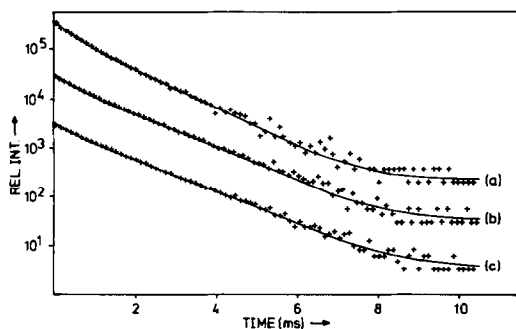


FIG. 4. Decay curves of the Eu^{3+} emission intensity in $\text{Na}_5\text{Gd}_{1-x}\text{Eu}_x(\text{WO}_4)_4$, $\lambda_{\text{exc}} = 527.62 \text{ nm}$, $\lambda_{\text{em}} = 617.65 \text{ nm}$. Solid lines discussed in text. (a) $x = 0.01$, $T = 4.2 \text{ K}$; (b) $x = 1$, $T = 4.2 \text{ K}$; (c) $x = 1$, $T = 80 \text{ K}$.

TABLE III
NUMBERS OF LINES OF THE ELECTRONIC TRANSITIONS IN THE LUMINESCENCE SPECTRA OF $\text{Na}_5\text{Eu}(\text{WO}_4)_4$

Excitation ${}^7F_0 \rightarrow$	5D_0	5D_1	5D_2			
Experiment	0	2	3			
S_4	0	2	3			
D_{2d}	0	2	2			
Emission ${}^5D_0 \rightarrow$	7F_0	7F_1	7F_2	7F_3	7F_4	
Experiment	0	2	2	1	3	
S_4	0	2	3	4	4	
D_{2d}	0	2	2	3	3	

The emission and excitation spectra show the well-known vibronic transitions which have been discussed elsewhere (3, 15, 16). Table I shows the ratio of the integrated intensities of the total vibronic sideband of the ${}^7F_0 \rightarrow {}^5D_2$ and ${}^5D_0 \rightarrow {}^7F_2$ transitions and the ${}^7F_0 \rightarrow {}^5D_1$ and ${}^5D_0 \rightarrow {}^7F_1$ magnetic-dipole transitions, respectively. The latter are taken as a standard, because their intensity is practically not influenced by changes in the surroundings of the Eu^{3+} ion.

The vibronic intensities are at least as strong as the magnetic-dipole intensities. In the emission spectra they do not depend on the Eu^{3+} concentration, but in the excitation spectra they do. For $\text{Na}_5\text{Eu}(\text{MoO}_4)_4$, which we measured to check our findings, the vibronic intensities are about equal to those for $\text{Na}_5\text{Eu}(\text{WO}_4)_4$.

The higher vibronic intensity in the excitation spectra, which seems to be a general feature (6, 17), points to a stronger coupling with the surroundings in the 7F ground state than in the 5D excited state (18). Hoshina *et al.* (19) have observed the same phenomena for Eu^{3+} in the oxysulfides, i.e., higher vibronic intensity in the excitation spectra and higher vibronic intensity for higher Eu^{3+} concentration. They suggested that the Eu^{3+} ions are coupled via the ${}^7\text{CTS}$ (charge-transfer state), which mixes with

the 7F ground state. This is not possible with the 5D excited state.

Since in our compounds the Eu^{3+} charge-transfer state and the tungstate charge-transfer state are more or less resonant, it is not clear what is the nature of the excited state which is mixed with the 7F state. The Eu^{3+} ions in $\text{Na}_5\text{Eu}(\text{WO}_4)_4$ are situated in the lattice in such a way that every Eu^{3+} ion has four Eu^{3+} nearest neighbors at a distance of 6.5 Å, separated from each other by a double $\text{Eu}-\text{O}-\text{W}-\text{O}-\text{Eu}$ bridge (7). This alignment, together with the Eu^{3+} -concentration dependence of the vibronic intensity, suggests that the excited state which mixes with 7F has at least a certain amount of tungstate character. It is an unexpected result that such weak transitions as the vibronic transitions under discussion can be influenced over such long distances. This shows that the tungstate groups play undoubtedly a role in the interaction mechanism.

According to considerations by Judd (20) the polarizability of the groups surrounding the rare-earth ion influences the vibronic intensity. The tungstate group is known to be rather well polarizable which seems to be a good reason why the vibronic transitions of Eu^{3+} in tungstates are so strong (16).

The concentration dependence of vibronic intensities has not been studied extensively. However, the examples of $\text{Ln}_{2-x}\text{Eu}_x\text{O}_2\text{S}$ (19) and $\text{Na}_5\text{Gd}_{1-x}\text{Eu}_x(\text{WO}_4)_4$ present clear evidence for such an effect. In a completely different way Auzel *et al.* (21) have shown that the vibronic interaction in the system $\text{Mg}_{1-x}\text{Ni}_x\text{F}_2$ increases with the concentration of the transition metal ion. For the rare-earth ions it is not so easy to perform the required measurements because the weak vibronics are most easily studied in excitation, but the luminescence intensity usually drops with increasing concentration. As such the system $\text{Na}_5(\text{Gd}, \text{Eu})(\text{WO}_4)_4$ is a favorable one. In order to confirm the present results we checked ear-

lier measurements on the system $(\text{Gd}, \text{Eu})_2(\text{MoO}_4)_3$ (3). The vibronics were given before. At 4.2 K the ratio given in Table I amounts to 10 for $\text{Eu}_2(\text{MoO}_4)_3$ and 4 for $(\text{Gd}_{0.99}\text{Eu}_{0.01})_2(\text{MoO}_4)_3$. These data refer to the excitation spectra and confirm the intensity dependence. In the solid solution series $(\text{Gd}, \text{Eu})_2(\text{MoO}_4)_3$ the rare-earth ions at different crystallographic sites between which energy transfer occurs (3) are 6.3 Å apart and separated by a similar double $\text{Eu}-\text{O}-\text{M}-\text{O}-\text{Eu}$ bridge as in $\text{Na}_5\text{Eu}(\text{WO}_4)_4$ (22), so that both systems are structurally and spectroscopically similar.

From the emission spectra it is not possible to derive such a ratio. They are complicated due to the presence of two crystallographic sites for the rare-earth ions. There is no doubt that the ratio in emission is much lower than in excitation. The ratio from the excitation spectra is very high, especially for the concentrated $\text{Eu}_2(\text{MoO}_4)_3$. Since this crystal structure shows ferroelectricity for several rare-earth ions (22) this confirms also the relation mentioned above between polarizability and vibronic intensity.

Let us now consider the vibrational frequencies involved. In Table II the frequencies derived from the vibronic transitions in the excitation and emission spectra are assigned to lattice and tungstate vibrations by comparing these with IR and Raman data given in Ref. (15). The ${}^5D_0 \rightarrow {}^7F_0$ electronic transition, which is not observed in the spectra due to its strongly forbidden character, is placed at 581.0 nm. This gives the best agreement between the vibrational frequencies involved and is in agreement with data given in Ref. (9). Vibronic coupling in tungstate compounds containing Eu^{3+} ions has been reported before (5, 9, 16). Our present results agree with these reports.

4.2. Energy Transfer Processes

The radiative decay time τ_0 of the Eu^{3+} ion in the $\text{Na}_5(\text{Gd}, \text{Eu})(\text{WO}_4)_4$ system was

determined from the exponential part of the decay curve of the diluted Eu^{3+} compound and found to be 760 μsec . From the fact that the decay curves of the concentrated compound have an exponential tail with the same time constant of 760 μsec , we can conclude that in $\text{Na}_5\text{Eu}(\text{WO}_4)_4$ energy migration over the Eu^{3+} sublattice to acceptor sites where the excitation energy is lost does not take place. Migration would result in an exponential decay with a time constant $\tau < \tau_0$ (23). The same observation has been made by Evdokimov *et al.* (10), who reported a Eu^{3+} decay time of 780 μsec for all samples in the dilution series $\text{Na}_5\text{La}_{1-x}\text{Eu}_x(\text{WO}_4)_4$.

The nonexponential initial part of the decay curves of $\text{Na}_5\text{Eu}(\text{WO}_4)_4$ reflects single-step energy transfer from Eu^{3+} donors (D) to acceptors (A), the nature of which is unknown. A theoretical description of the time development of the donor luminescence intensity in the case of single-step D–A transfer without D–D transfer has been given by Inokuti and Hirayama (24). In their model they assume an isotropic distribution of the D and A centers over the lattice, absence of A–D backtransfer, and D–A interaction of the multipole–multipole type. They derived the expression

$$I(t) = I(0)\exp[-t/\tau_0 - \Gamma(1 - 3/s)(N_A/N_0)(t/\tau_0)^{3/s}], \quad (1)$$

in which $s = 6, 8, 10, \dots$ dependent on the type of multipolar D–A interaction, N_A is the acceptor concentration, and N_0 is the critical acceptor concentration, given by

$$N_0^{-1} = 4/3\pi R_c^3 \quad (2)$$

Here R_c is the critical distance for energy transfer for which the donor radiative rate $P_{\text{rad}} (= 1/\tau_0)$ equals the D–A transfer rate P_{DA} . The decay curves of the diluted and the concentrated composition could be fitted very well to Eq. (1). Some examples are

given in Fig. 4, where the solid lines represent a fit to Eq. (1) assuming dipolar D–A interaction ($s = 6$).

Using the measured decay curve of $\text{Na}_5\text{Eu}(\text{WO}_4)_4$ at 4.2 K, we estimate the amount of Eu^{3+} ions which are responsible for the nonexponential initial part of the decay, i.e., whose luminescence is influenced by single-step transfer to acceptors, to be about 6%. In the diffuse reflectance spectrum of $\text{Na}_5\text{Eu}(\text{WO}_4)_4$ there is a very weak, broad absorption band between 440–640 nm, which may be due to the acceptors. A possible explanation for this may be that the Na:Eu ratio deviates slightly from 5:1, which can be compensated by the presence of Eu^{2+} : $\text{Na}_{5-\delta}(\text{Eu}^{2+})_{2\delta}(\text{Eu}^{3+})_{1-\delta}(\text{WO}_4)_4$. Between Eu^{2+} and WO_4^{2-} a charge-transfer transition can occur.

If this assumption is correct, the critical transfer distance R_c for the transfer $\text{Eu}^{3+} \rightarrow \text{A}$ is estimated to be about 30 Å, following a procedure described in Ref. (25) (see also Eq. (3)). The Eu^{3+} ions which are at a short distance from A are completely quenched. We assume that the 6% of the Eu^{3+} ions which cause the nonexponential initial part of the decay curve are located between 20 and 30 Å from an acceptor site. This means that about 10% of all Eu^{3+} ions are within 30 Å of an acceptor. From this the acceptor concentration is estimated to be 0.03% of the Eu^{3+} ions. Compared to other concentrated compounds (1, 2, 26), this is a relatively low value. This may be the reason why the concentration quenching in the solid solution series is inefficient: during its radiative lifetime the excitation energy of the Eu^{3+} ions cannot reach an acceptor site; i.e., the Eu^{3+} – Eu^{3+} transfer rate P_{DD} is too small to compete with P_{rad} , and multistep energy migration is not observed up to room temperature.

From this observation we conclude that the interactions between the Eu^{3+} ions are very weak. According to the theory of energy transfer, these interactions can be

multipolar–multipolar or exchange in character (27).

Let us first consider exchange interactions. The Eu^{3+} nearest neighbor distance (6.5 Å) is too large for effective direct exchange interaction (26). In crystals of the system $(\text{Gd}, \text{Eu})_2(\text{MoO}_4)_3$ energy transfer takes place over a distance of 6.3 Å by superexchange interactions via the O–M–O bridges that link the Eu^{3+} ions (3). However, in powder samples of the same system no energy migration could be demonstrated, probably because of a higher purity of the samples (28). Considering the small amount of impurities in $\text{Na}_5\text{Eu}(\text{WO}_4)_4$, this may be a comparable case. P_{DD} via superexchange interactions across the O–W–O bridges cannot compete with P_{rad} .

We can compare this with $(\text{Gd}, \text{Eu})\text{NbO}_4$ (6). In this system superexchange interactions are probably active across a niobate group intermediary over a distance of 7.4 Å. The Eu–O–Nb–O–Eu angle is about 180°. In $\text{Na}_5\text{Eu}(\text{WO}_4)_4$ the Eu–O–W–O–Eu angle is about 120°, which is less favorable for superexchange interaction (29). This results in a lower P_{DD} than in $(\text{Gd}, \text{Eu})\text{NbO}_4$ despite the shorter Eu^{3+} – Eu^{3+} distance.

Now we turn to multipolar interactions. At low temperatures the multipolar interaction between the Eu^{3+} ions has to take place via the 7F_0 – 5D_0 electric dipole transition. This transition is absent in the spectra of $\text{Na}_5\text{Eu}(\text{WO}_4)_4$, which indicates that energy migration via dipole–dipole interaction is very improbable. At higher temperatures the 7F_1 state of Eu^{3+} becomes thermally populated. Energy migration can then occur via the 7F_1 – 5D_0 transition, as has been encountered in $\text{EuAl}_3\text{B}_4\text{O}_{12}$ (30) and $\text{Eu}(\text{IO}_3)_3$ (12). In these compounds the Eu–Eu distance is somewhat smaller (≈ 6 Å) than in $\text{Na}_5\text{Eu}(\text{WO}_4)_4$ (6.5 Å). Also, the lowest 7F_1 level in these compounds lies at an energy of 225 and 250 cm^{-1} above 7F_0 , respectively. In $\text{Na}_5\text{Eu}(\text{WO}_4)_4$ the 7F_1 crystal field splitting is small ($\approx 50 \text{ cm}^{-1}$), and the

lowest 7F_1 level lies at 350 cm^{-1} above the 7F_0 ground state (9). This higher activation energy for the migration via ${}^7F_1-{}^5D_0$, together with the larger Eu–Eu distance, are expected to result in a low value of P_{DD} .

Having considered the energy transfer between Eu^{3+} and acceptors and between the Eu^{3+} ions mutually, we now turn to energy transfer from the WO_4^{2-} group to the Eu^{3+} ions. This is a very efficient process, considering the small amount of WO_4^{2-} emission in the spectra of $\text{Na}_5\text{Eu}(\text{WO}_4)_4$ after WO_4^{2-} excitation. The critical distance R_c for the $\text{WO}_4^{2-} \rightarrow \text{Eu}^{3+}$ transfer can be estimated using the emission spectrum of $\text{Na}_5\text{Gd}(\text{WO}_4)_4$ (Fig. 1) via the procedure described in Ref. (25):

$$R_c^6 = 6.3 \times 10^{27} \times \frac{4.8 \times 10^{-16}}{E^4} \times f \times SO. \quad (3)$$

Here f is the oscillator strength of the ${}^7F_0 \rightarrow {}^5D_2$ transition of Eu^{3+} ($\approx 10^{-7}$), SO is the normalized spectral overlap ($\approx 1.2\text{ eV}^{-1}$), and E is the energy of maximum spectral overlap between Eu^{3+} absorption and WO_4^{2-} emission ($= 2.7\text{ eV}$). With Eq. (3) we assume electric dipole–dipole interaction between WO_4^{2-} and Eu^{3+} . The given values lead to $R_c \approx 4.3\text{ \AA}$. This is larger than the actual W–Eu distance (3.9 \AA), which explains why the transfer $\text{WO}_4^{2-} \rightarrow \text{Eu}^{3+}$ is an efficient process.

Following the same procedure, it becomes clear why the transfer process $\text{Gd}^{3+} \rightarrow \text{WO}_4^{2-}$ in $\text{Na}_5\text{Gd}(\text{WO}_4)_4$ is inefficient. The spectral overlap of the Gd^{3+} emission at 312 nm and the WO_4^{2-} excitation band is very small. This explains the presence of the Gd^{3+} absorption as a negative peak on the WO_4^{2-} excitation band. The WO_4^{2-} emission observed after excitation of the ${}^8S \rightarrow {}^6I$ Gd^{3+} transition must be due to partial absorption of the exciting radiation by the tungstate groups.

5. Conclusions

The concentration dependence of the vibronic intensity in the excitation spectra of $\text{Na}_5(\text{Gd, Eu})(\text{WO}_4)_4$ can be explained by assuming a tentative model which involves mixing of the 7F and ${}^7\text{CTS}$ of the Eu^{3+} ion with the CTS of the WO_4^{2-} group. Energy migration in $\text{Na}_5\text{Eu}(\text{WO}_4)_4$ is not observed due to the fact that electric dipole–dipole and superexchange interactions between the Eu^{3+} ions are too weak to result in efficient migration to acceptor sites. Single-step energy transfer occurs from Eu^{3+} to acceptors and from WO_4^{2-} to Eu^{3+} .

Acknowledgments

The authors thank Mrs. C. Dorland and M. Boeren for preparing some of the samples and performing part of the measurements. The investigations were supported by the Netherlands Foundation for Chemical Research (SON) with financial aid from the Netherlands Organization for Scientific Research (NWO).

References

1. P. A. M. BERDOWSKI AND G. BLASSE, *J. Lumin.* **29**, 243 (1984).
2. P. A. M. BERDOWSKI, J. VAN HERK, AND G. BLASSE, *J. Lumin.* **34**, 9 (1985).
3. M. BUIJS, G. BLASSE, AND L. H. BRIXNER, *Phys. Rev. B* **34**, 8815 (1986).
4. M. BUIJS AND G. BLASSE, *J. Lumin.* **39**, 323 (1988).
5. J. P. M. VAN VLIET, G. BLASSE, AND L. H. BRIXNER, *J. Solid State Chem.* **76**, 160 (1988).
6. J. P. M. VAN VLIET, D. VAN DER VOORT, AND G. BLASSE, *J. Lumin.* **42**, 305 (1989).
7. L. G. SILLÉN AND H. SUNDVALL, *Arkiv. Kem. Mineral. Geol. A* **17**, 10 (1943).
8. V. A. EFREMOV, T. A. BEREZINA, I. M. AVERINA, AND V. K. TRUNOV, *Sov. Phys. Crystallogr.* **25**, 146 (1980).
9. J. HUANG, J. LORIER, P. PORCHER, G. TESTE DE SAGEY, P. CARO, AND C. LEVY-CLEMENT, *J. Chem. Phys.* **80**, 6204 (1984).
10. A. A. EVDOKIMOV, V. K. TRUNOV, T. A. BEREZINA, E. V. VASIL'EV, AND V. K. ISHUNIN, *Russ. J. Inorg. Chem.* **24**, 519 (1979).

11. J. PAN, L. YAU, L. CHEN, G. ZHAO, G. ZHOU, AND C. GUO, *J. Lumin.* **40**, **41**, 856 (1988).
12. J. P. M. VAN VLIET, G. BLASSE, AND L. H. BRIXNER, *J. Electrochem. Soc.* **135**, 1574 (1988).
13. A. J. DE VRIES, J. P. M. VAN VLIET, AND G. BLASSE, *Phys. Stat. Sol. (b)* **149**, 391 (1988).
14. G. BLASSE, *Struct. Bond.* **42**, 1 (1980).
15. P. TARTE AND M. LIEGEOIS-DUYCKAERTS, *Spectrochim. Acta A* **28**, 2029, 2037 (1972).
16. N. YAMADA AND S. SHIONOYA, *J. Phys. Soc. Japan* **31**, 841 (1971).
17. G. BLASSE, to be published.
18. B. DiBARTOLO, "Optical Interactions in Solids," Sect. 16.3, Wiley, New York (1968).
19. T. HOSHINA, S. IMANAGA, AND S. YOKONO, *J. Lumin.* **15**, 455 (1977).
20. B. R. JUDD, *Phys. Scr.* **21**, 543 (1980).
21. F. AUZEL, J. M. BRETEAU, AND D. MEICHENIN, *J. Lumin.* **40**, **41**, 595 (1988).
22. L. H. BRIXNER, J. R. BARKLEY, AND W. JEITSCHKO, in "Handbook on the Physics and Chemistry of Rare Earths" (K. A. Geschneidner and L. Eyring, Eds.), Vol. 3, Chap. 30, North-Holland, Amsterdam (1979).
23. D. L. HUBER, in "Laser Spectroscopy of Solids" (W. M. Yen and P. M. Selzer, Eds.), Chap. 3, Springer-Verlag, Berlin (1981).
24. M. INOKUTI AND F. HIRAYAMA, *J. Chem. Phys.* **43**, 1978 (1965).
25. G. BLASSE, *Mater. Chem. Phys.* **21**, 201 (1987).
26. M. BUIJS AND G. BLASSE, *J. Lumin.* **34**, 263 (1986).
27. D. L. DEXTER, *J. Chem. Phys.* **21**, 836 (1953).
28. M. OUWERKERK, F. KELLENDONK, AND G. BLASSE, *J. Chem. Soc., Faraday Trans. 2*, 78 (1982).
29. G. BLASSE, *Proc. Int. Conf. Magn. IOP, London*, 350 (1964); *Philips Res. Rep.* **20**, 327 (1965).
30. F. KELLENDONK AND G. BLASSE, *J. Chem. Phys.* **75**, 561 (1981).